J Biomed Mater Res 64A: 114–119, 2003

# Low permeability biomedical polyurethane nanocomposites

**Ruijian Xu,[1] Evangelos Manias,[1] Alan J. Snyder,[2] James Runt[1]**
[1]*Department of Materials Science and Engineering, and Materials Research Institute, The Pennsylvania State University, University Park, Pennsylvania 16802*
[2]*Department of Surgery, College of Medicine, The Milton S. Hershey Medical Center, The Pennsylvania State University, Hershey, Pennsylvania 17033*

Received 25 October 2001; accepted 8 April 2002

**Abstract:** In this article we describe our continuing research on a novel nanocomposite approach for reducing gas permeability through biomedical polyurethane membranes. Nanocomposites were prepared using commercially available poly(urethane urea)s (PUU) and two organically modified layered silicates (OLS). Wide-angle X-ray diffraction experiments showed that the silicate layer spacing in the nanocomposites increased significantly compared with the neat OLS, signifying the formation of intercalated PUU/OLS structures. The nanocomposite materials exhibit increased modulus with increasing OLS content, while maintaining polymer strength and ductility. Water vapor permeability was reduced by about fivefold at the highest OLS contents, as a result of PUU/inorganic composite formation. © 2002 Wiley Periodicals, Inc. J Biomed Mater Res 64A: 114–119, 2003

**Key words:** polyurethane; nanocomposite; permeability; cardiac assist device; membrane

## INTRODUCTION

Segmented polyurethanes, and in particular poly(urethane urea)s (PUUs), are currently used in a variety of blood-contacting applications in biomedical devices. For example, the Arrow International LionHeart and Abiomed's AbioCor cardiac assist devices utilize PUU elastomers in the blood pump as well as in other locations. In general, biomedical PUUs possess good biocompatibility and flexural fatigue characteristics but, because of the low $T_g$ and relatively high concentration of soft segments, are relatively permeable to air and water vapor. The latter can lead to potential problems, particularly in completely implantable devices.

The traditional approach to this problem is to modify the chemistry of the copolymer, particularly that of the soft segment. For example, replacement of the usual polytetramethylene oxide (PTMO) soft segments with aliphatic polycarbonate segments results in twofold reduction in water vapor transmission rate compared with PTMO-based counterparts.[1] We have recently taken an alternative approach that involved the synthesis of comb polymers in which small comb branches of relatively low permeability polyisobutylene (PIB) are "grafted" on a PTMO soft segment PUU backbone.[2] This approach was used because attempts of substituting the polyether soft segments with PIB resulted in low overall copolymer molecular weight and poor mechanical properties.[3] In order to synthesize the comb polymers, it was first necessary to synthesize end-functionalized PIB macromonomers containing a diol functionality, $(-OH)_2$, on one end of the molecule. This was accomplished using a new polymerization initiator and pseudo-cationic polymerization.[2] Several series of comb polymers were synthesized from methylene bis(*p*-phenyl isocyanate) (MDI), ~2000 molecular weight PTMO, ethylene diamine (EDA) and one of four PIB diols having molecular weights ranging from ~3,000 to 29,000. Hard segment concentration was maintained at ~22 wt% for all comb polymers. However, even at the highest PIB contents, only a modest (twofold) reduction in water vapor and oxygen permeability was observed, because of the lack of control over the phase-separated morphology of the PIB microdomains.[4]

Recently, a more efficient approach for reducing the permeability of elastomers has received widespread attention. The basic idea is to disperse an organically modified layered silicate (OLS) in the polymer, creating a more tortuous path for diffusion of gas molecules through the composite. Provided that the inor-

*Correspondence to:* J. P. Runt; e-mail: runt@matse.psu.edu
Contract grant sponsor: Arrow International.
Contract grant sponsor: National Heart, Lung, and Blood Institute of the National Institutes of Health; contract grant number: contract N01-HV-58156.

© 2002 Wiley Periodicals, Inc.

ganic OLS layers are finely dispersed throughout the polymer (see below) during processing, the permeability of the resulting nanocomposite can be substantially reduced (as a result of the relatively high aspect ratio of the impermeable silicates layers), even at modest OLS concentrations.[5–7] In a recent publication[8] we demonstrated the utility of this approach for biomedical PUUs, realizing as much as a fivefold reduction in water vapor permeability at relatively low OLS loadings. This nanocomposite approach is generally applicable to a wide range of polymers, and in this article we present an extension of this work to commercial PUUs that are used in cardiac assist devices.

## EXPERIMENTAL

### Materials and nanocomposite preparation

The two commercial biomedical PUUs used in this study were obtained from the Polymer Technology Group: BioSpan and BioSpan MS/0.4. BioSpan has been recognized by the FDA as a Biomer replacement and has been used in a substantial number of clinical ventricular assist and artificial heart devices. Although the exact compositions of these segmented block copolymers are proprietary, BioSpan is prepared from MDI, ~2000 molecular weight PTMO and mixed diamine chain extenders [EDA and 1,3-cyclohexanediamine (1,3-CHD)].[9] The hard segment concentration of this copolymer is ~20 wt%. The chemistry of BioSpan MS/0.4 is similar, except that a portion of the chain ends are capped with ~2000 molecular weight poly(dimethylsiloxane) to a level of 0.4 wt% of the copolymer. In addition, both polymers contain ~5% of a polymethacrylate modifier that is immiscible with the PUU copolymer. The standard quantity (ca. 1%) of antioxidant was present in each. Both polymers were received in ~20 wt% solution in *N,N*-dimethylacetamide (DMAc).

The two organically modified layered silicates used in our experiments were Cloisite 15A (Southern Clay Products) and Nanomer I.30TC (Nanocor). The former material was prepared by the supplier by ion-exchanging $Na^+$ montmorillonite (MMT) with dimethyl ditallow ammonium. The tallow used was composed of ca. 65% $C_{18}$, 30% $C_{16}$, and 5% $C_{14}$ units and is introduced in excess of the cation exchange capacity to approximately 1.25 meq/g. Nanomer I.30TC was also prepared by the supplier, by ion-exchanging $Na^+$ MMT with octadecylammonium. The average aspect ratios ($\alpha$) of Cloisite 15A and Nanomer I.30TC have been reported by the manufacturers to be 200–500. Both OLS were used as received.

Because Cloisite 15A does not disperse efficiently in DMAc, a 3 wt% transparent solution of this OLS in toluene was prepared, then added dropwise to a 3 wt% solution of BioSpan in DMAc, and stirred for 3 h at 80°C. The mixture was then stirred overnight at room temperature. The solution was degassed, then films were cast onto round glass petri dishes. The films were air dried for 24 h and subsequently dried under vacuum at 50°C for 24 h. Composites containing final concentrations of 1, 3, 7, 13, and 20 wt% OLS were prepared. Assuming that the hydrocarbon surfactant and neat silicate have densities of 0.8 and 2.5 g/mL respectively, these OLS weight fractions correspond to ~0.3, 0.8, 2.0, 3.8, and 5.9 vol% inorganic layered silicates, respectively.

Because of the different organic modification, Nanomer I.30TC disperses well in DMAc, forming a transparent 3 wt% solution. This solution was added dropwise to a 10 wt% solution of BioSpan MS/0.4 in DMAc and stirred for 3 h at 80°C. The remainder of the film preparation and drying procedure was the same as for the Cloisite 15A nanocomposites. Final films containing 10 wt% OLS were quite transparent, indicating good OLS dispersion in the solid state. A schematic of our nanocomposite preparation procedure is shown in Figure 1.

### Characterization

X-ray diffraction experiments were performed on film samples on a Rigaku X-ray diffractometer operating in a theta-theta geometry using Cu $K_\alpha$($\lambda$ = 0.154 nm) radiation. Samples were scanned at a rate of 1°/min from ~1.5–40° 2$\theta$, using a step size of 0.02°. Diffraction patterns of the OLS powders were obtained by loading each into the cavity of an aluminum sample holder and compacting the powder with a glass plate until a smooth surface was obtained.

Evaluation of the mechanical properties was carried out on a table model Instron tensile testing machine on specimens cut with a microtensile die (ASTM D1708-93). A crosshead speed of 100 mm/min was used for all experiments. Ultimate strength ($\sigma_b$) and elongation ($\varepsilon_b$) as well as the modulus at 50% extension ($E_{50}$) were determined from five specimens taken from each of the composites. Mean values and their standard deviations are reported in the tables.

Water vapor permeability of the nanocomposite films (0.25 mm thick) was determined at 27°C according to ASTM E96-95. Dry films were sealed to the open mouths of test bottles containing desiccant (anhydrous calcium sulfate) and placed in a chamber controlled at 90% relative humidity. Periodic weighings of the assembly allow for the determination of water vapor transmission rate, from which the permeability is calculated.

Fourier transform infrared spectroscopy (FTIR) and differential scanning calorimetry (DSC) experiments were also conducted on selected BioSpan–Cloisite 15A nanocomposites. For the FTIR experiments, thin films were deposited on KBr disks. The spectra were acquired in transmission using a Biorad FTS 45 spectrometer. Each sample was scanned 64 times at a resolution of 2 $cm^{-1}$, and the scans were signal averaged. All spectral absorbances fall within the range of Beer's Law. For presentation purposes each spectrum was first normalized using the area of the 1412 $cm^{-1}$ peak, assigned to the C–C stretching mode of the aromatic ring.[10]

A Seiko Instruments DSC 220 CU equipped with a liquid nitrogen cooling tank was used in this study. Samples were first heated at 20°C/min to 120°C and then cooled to −120°C and reheated to 150 (or 200)°C. Data were recorded on heating from −120°C. PUUs like BioSpan and BioSpan MS/0.4

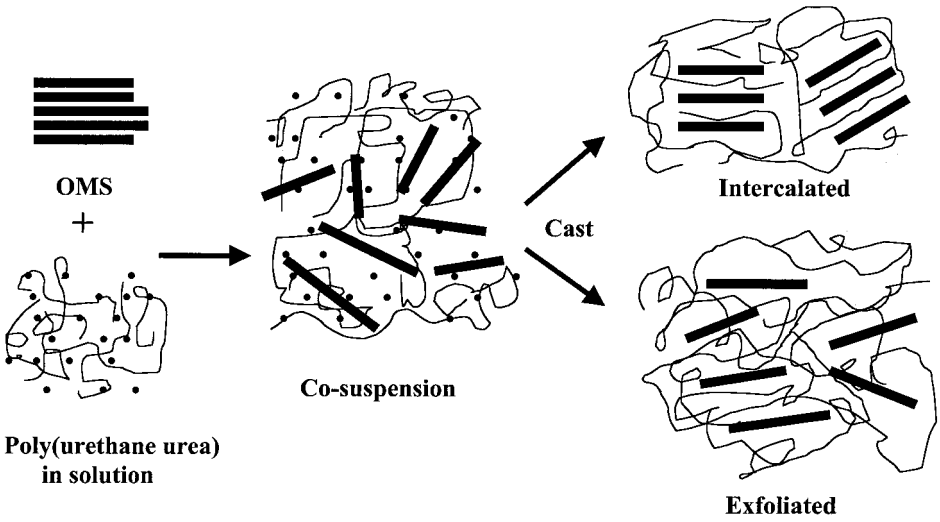


**Figure 1.** Schematic drawing of the preparation of the BioSpan and BioSpan MS/0.4 nanocomposites. The black circles represent solvent molecules; the lines, PUU chains; and the "blocks" a single silicate layer. The relative size of the blocks are for illustrative purposes only and the relative dimensions do not represent those of a single silicate layer (~1 nm thick and having an aspect ratio of ~200–500).

cannot be heated for a significant time period above 150°C without chemical changes occurring in the polymer.[11] Consequently, the DSC experiments can only be used to characterize soft phase transitions and any relatively low temperature hard phase transitions.

## RESULTS AND DISCUSSION

The X-ray diffraction patterns of the BioSpan–Cloisite 15A and BioSpan MS/0.4–Nanomer I.30TC nanocomposites are presented in Figures 2 and 3, respectively. The neat BioSpan polymers exhibit an amorphous halo near 20° 2θ, consistent with our studies on similar PUUs,[11] and is found at the same location for all of the composites. The spacing between silicate layers ($d_{001}$) of the unmodified $Na^+$ MMT (not shown in Fig. 2) was determined to be 1.2 nm. Incorporating organic species on the silicate surfaces increases the layer spacing in Cloisite 15A to 2.8 nm. This increases further (to about 3.4 nm) for all of the BioSpan–Cloisite 15A composites. Similar behavior is seen in Figure 3 for the BioSpan MS/0.4–Nanomer I.30TC mixtures: the gallery spacing increases from 2.5 nm for Nanomer I.30TC to ~3.2–3.4 nm for the nanocomposites. These results clearly show that the PUU copolymers are intercalated/inserted between the silicate layers, and some of them readopt a parallel registry after solvent evaporation. Finally, the absence of any diffraction peaks at the characteristic d-spacings of the organo-MMT demonstrate that all the layers are dispersed in the polymer matrix (resulting in intercalated or exfoliated structures). Second- and third-order (002 and 003) reflections are also observed at higher silicate loadings.

The role of the nonpolar alkyl ammonium cations in the OLS is generally to lower the surface energy of the native MMT and improve wetting with selected polymers. Confinement of polymer chains in the silicate galleries results in a decrease in entropy but this may be at least partially compensated for by an increase in conformational freedom of the end-grafted alkyl surfactants when the layers separate.[12] Because changes in interlayer spacing are generally modest, at equilibrium, the change in system enthalpy will determine if intercalation is possible from a thermodynamic perspective.[12] Like the present situation in which the polymer and OLS layers are in solution and films are formed by casting, kinetic trapping of the OLS layers by polymer chains is also a possibility.[13]

Favorable enthalpy for silicate–PUU mixing could arise from polar or hydrogen bonding interactions between C=O and N–H in the PUU chains (hard seg-

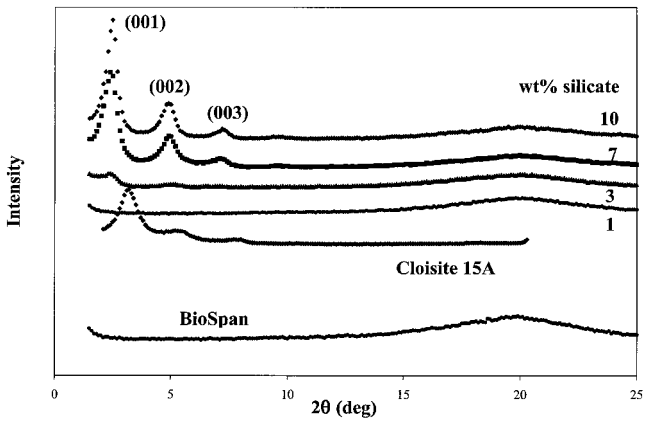


**Figure 2.** X-ray diffraction patterns of BioSpan, Cloisite 15A and selected BioSpan–Cloisite 15A nanocomposites

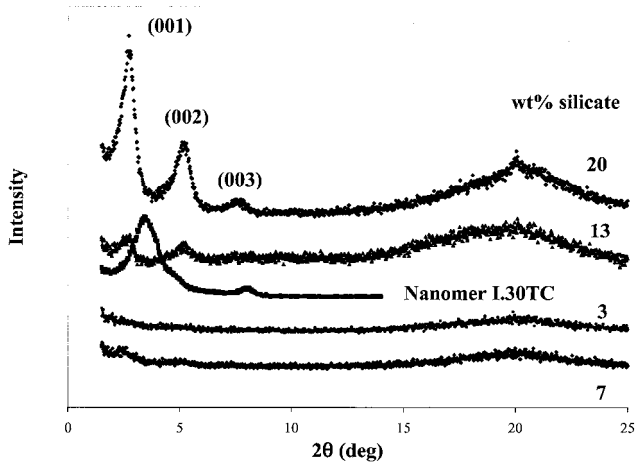


**Figure 3.** X-ray diffraction patterns of Nanomer I.30TC, BioSpan MS/0.4, and selected BioSpan MS/0.4–Nanomer I.30TC nanocomposites

ment) and polar sites on the silicate surface (the grafting density of alkyl species resulting from cation exchange is on the order of one surfactant molecule per 174 Å$^2$). Potential sites on the silicate layer surfaces for polar or hydrogen bonding interactions become increasingly accessible as the layers are separated. The FTIR spectra of PUUs (and diol-based polyurethanes) are well known to be sensitive to hard domain organization and the urea and urethane hydrogen bonding.[10,14–17] Consequently, we compared the FTIR spectra of the BioSpan–Cloisite 15A nanocomposites with those of the neat components. We focused primarily on the carbonyl (~1620–1760 cm$^{-1}$) and N–H stretching (3150 and 3500 cm$^{-1}$) regions. Even at the highest OLS contents, no discernable changes in the spectra of the nanocomposites compared with that of BioSpan were observed. This is illustrated in Figure 4 for composites containing 20 and 30 wt% Cloisite 15A. Consequently, the FTIR data available at this point suggest that dispersed OLS layers in the PUU matrix are kinetically trapped.

DSC thermograms for the BioSpan–Cloisite 15A composites are shown in Figure 5. The soft phase glass transition temperatures of all nanocomposites are the same as that of the neat BioSpan (about −68°C). In addition, the heats of fusion of crystalline soft segments (that crystallized on cooling to subambient temperatures), normalized to the PUU weight in the mixtures, were also found to be independent of OLS content (~25 J/g). Thus, the crystallization of the soft segments is not modified in the vicinity of the silicate surfaces, which is characteristic of polymers (or segments of block copolymers) with weak interactions with MMT fillers (such as polypropylene[18]). In contrast, for polymers with strong specific interactions with the surfaces [such as nylon 6[19] and poly(vinylalcohol)[13]] the filler nucleates crystal structures that differ from those in the bulk polymers.

The tensile mechanical properties of both types of nanocomposites are summarized in Tables I and II. When inorganic fillers are dispersed in polymers, elastic modulus is typically increased, with a concurrent sacrifice of the ultimate strength and elongation. Not surprisingly, for our composites, the nanodispersed silicates result in a significant increase in modulus (by

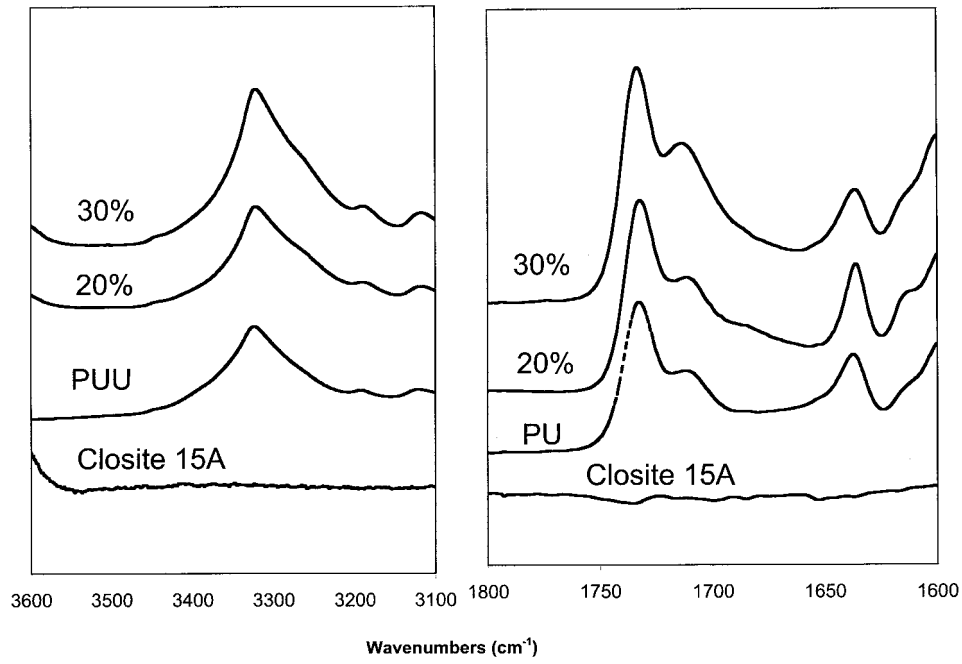


**Figure 4.** FTIR spectra of BioSpan, Cloisite 15A, and 20 and 30 wt% BioSpan–Cloisite 15A nanocomposites from 3100 and 3600 cm$^{-1}$ and 1600–1800 cm$^{-1}$.

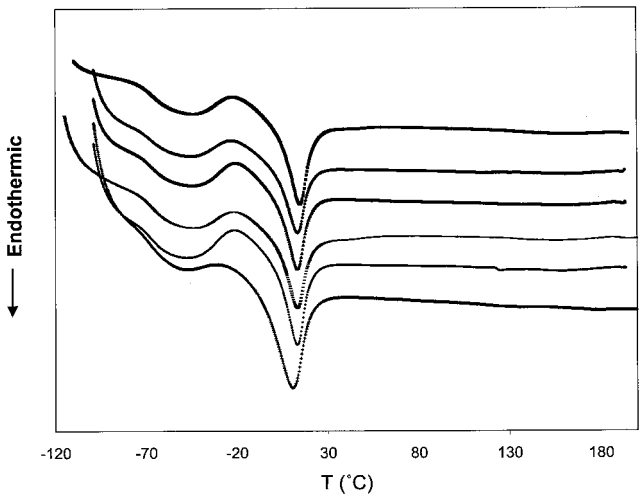


**Figure 5.** DSC thermograms of BioSpan and BioSpan–Cloisite 15A nanocomposites. Bottom to top, respectively: Biospan, 1%, 3%, 7%, 13%, and 20% composites.

a factor of 2–3 at 20 wt% OLS); however, the ultimate strength remains comparable to that of the neat PUUs or is perhaps in excess of that for some compositions. Remarkably, these changes are also accompanied by retention of the native PUU ductility, maybe even an increase in strain to failure at relatively low OLS levels.[8] A clear picture of the micromechanics of the silicate–PUU "interaction" that leads to this remarkable behavior has not yet emerged.[20,21] Although in the bulk state silicates behave as relatively rigid materials, transmission electron micrographs of nanocomposite morphology show that individual silicate layers, because of their high aspect ratio and nanometer thickness, exhibit a measure of flexibility.[22]

The water vapor permeabilities of both series of nanocomposites are presented in Figure 6 in terms of $P_C/P_0$, i.e., the permeability of the nanocomposite ($P_C$) relative to that of the unfilled BioSpan or BioSpan MS/0.4 polymers ($P_0$). Note that there is a very significant reduction in permeability: reaching about fivefold at the highest OLS contents, considerably larger than what is typically achieved by chemical modification of polyurethanes.[1,2] As noted earlier, this is a consequence of the more tortuous path required for the penetrant molecules to permeate through the membrane. Reduction in water vapor permeability is similar for the two series of materials, with the I.30TC OLS perhaps a bit more effective at lower OLS concentrations.

**TABLE I**
**Mechanical Properties of BioSpan–Cloisite 15A Nanocomposites**

| OLS Loading (wt%) | Modulus at 50% Strain $E_{50}$ (psi) | Ultimate Strength $\sigma_b$ (psi) | Ultimate Elongation $\varepsilon_b$ (%) |
|---|---|---|---|
| 0 | 510 (±40) | 4280 (±340) | 820 (±60) |
| 1 | 620 (±60) | 4860 (±310) | 1010 (±80) |
| 3 | 740 (±70) | 4770 (±410) | 900 (±90) |
| 7 | 900 (±70) | 5150 (±290) | 860 (±70) |
| 13 | 1190 (±70) | 4540 (±290) | 830 (±60) |
| 20 | 1370 (±80) | 4410 (±270) | 800 (±100) |

**TABLE II**
**Mechanical Properties of BioSpan MS/0.4–Nanomer I.30TC Nanocomposites**

| OLS Loading (wt%) | Modulus at 50% Strain $E_{50}$ (psi) | Ultimate Strength $\sigma_b$ (psi) | Ultimate Elongation $\varepsilon_b$ (%) |
|---|---|---|---|
| 0 | 540 (±50) | 4500 (±350) | 890 (±60) |
| 3 | 760 (±60) | 5550 (±450) | 1100 (±80) |
| 7 | 880 (±40) | 5400 (±220) | 980 (±60) |
| 13 | 1100 (±80) | 4800 (±250) | 870 (±50) |
| 20 | 1410 (±70) | 4450 (±240) | 850 (±110) |

The solid lines in Figure 6 represent predictions for the permeability through the thickness of a composite film that has dispersed, completely oriented, impenetrable filler layers. In the dilute and semidilute regimes[23,24]:

$$P_C/P_0 = (1 + \mu\alpha^2\phi^2)^{-1} \quad (1)$$

where $\phi$ is the filler volume fraction, $\alpha$ the filler aspect ratio and $\mu$ a "geometric factor," [24] $\mu = \pi^2/16\ln^2\alpha$. Comparison between the experimental values and model predictions suggests a gradual change in the effective aspect ratio of the silicate filler particles: a change from high aspect ratio exfoliated single layers at low loadings, to intercalated multilayer stacks of smaller effective aspect ratios at higher volume fractions.

## SUMMARY

We report on our continuing investigation of a novel nanocomposite approach for significantly re-

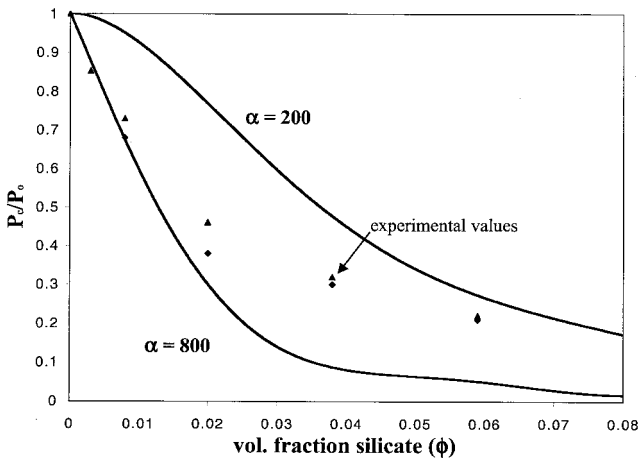


**Figure 6.** Relative water vapor permeability for BioSpan–Cloisite 15A (▲) and BioSpan MS/0.4–Nanomer I.30TC (◆) nanocomposites. The solid lines represent predictions from Eq. 1 for aspect ratios = 200 and 800.

ducing the permeability of biomedical polyurethanes. The water vapor permeabilities of composites prepared from commercially available PUUs and organically modified silicates were reduced by as much as a factor of five, as a result of nanoscale dispersion of the OLS. The stiffness of the nanocomposites was found to increase between two- and threefold up to 20 wt% OLS loading, whereas the ultimate strength remained approximately constant. The enhancement of permeability and modulus is achieved *without* loss of ductility. Such enhancements are beyond what can be generally achieved by chemical modification of polyurethanes. Further efforts are planned to confirm biocompatibility and assess high cycle fatigue resistance of the nanocomposites.

The authors thank Kenneth Strawhecker for helpful discussions and assistance. The authors also thank Arrow International and the National Heart, Lung and Blood Institute of the National Institutes of Health (contract N01-HV-58156) for support of this research.

## References

1. Yang M, Zhang Z, Hahn C, Laroche G, King MW, Guidoin R. Totally implantable artificial hearts and left ventricular assist devices: selecting impermeable polycarbonate urethane to manufacture ventricles. J Biomed Mater Res Appl Biomater 1999;48:13–33.
2. Weisberg DM, Gordon B, Rosenberg G, Snyder AJ, Benesi A, Runt J. Synthesis and characterization of amphiphilic poly(urethaneurea)–*comb*–polyisobutylene copolymers. Macromolecules 2000;33:4380–4389.
3. Yeh J, Gordon B, Rosenberg G. Moisture diffusivity of biomer versus biomer-coated polyisobutylene polyurethane urea (pib-puu)—a potential blood sac material for the artificial heart. J Mater Sci Lett 1994;13:1390–1391.
4. Weisberg DM, Garrett JT, Siedlecki C, Rosenberg G, Snyder AJ, Runt J. 2002. Manuscript in preparation.
5. Alexander M, Dubois P. Polymer-layered silicate nanocomposites: preparation, properties and uses of a new class of materials. Mater Sci Eng 2000;R28:1–63.
6. LeBaron PC, Wang Z, Pinnavaia TJ. Polymer-layered silicate nanocomposites: an overview. J Appl Clay Sci 1999;15:11–29.
7. Giannelis EP, Krishnamoorti RK, Manias E, Polymer-silicate nanocomposites. Adv Polym Sci 1998;138:107–148.
8. Xu R, Manias E, Snyder AJ, Runt J. New biomedical poly(urethane urea)–layered silicate nanocomposites. Macromolecules 2001;34:337–339.
9. Wen J, Somorjai G, Lim F, Ward RS. XPS study of surface composition of a segmented polyurethane copolymer modified by pdms end groups and its blends with phenoxy. Macromolecules 1997;16:7206–7213.
10. McCarthy SJ, Meijs GF, Mitchell N, Gunatillake PA, Heath G, Brandwood A, Schindhelm K. In-vivo degradation of polyurethanes: transmission-ftir microscopic characterization of polyurethanes sectioned by cryomicrotomy. Biomaterials 1997; 18:1387–1409.
11. Garrett JT, Lin JS, Runt J. Influence of preparation conditions on microdomain formation in poly(urethane urea) block copolymers. Macromolecules 2002;35:161–168.
12. Vaia RA, Giannelis EP. Lattice model of polymer melt intercalation in organically-modified layered silicates. Macromolecules 1997;30:7990–7999.
13. Strawhecker K, Manias E. Structure and properties of poly(vinyl alcohol)/montmorillonite nanocomposites. Chem Mater 2000;12:2943–2949.
14. Wang CB, Cooper SL. Morphology and properties of segmented polyether polyurethaneureas. Macromolecules 1983; 16:775–786.
15. Sung CSP, Smith TW, Sung NH. Properties of segmented polyether poly(urethaneurea)s based on 2,4-toluene diisocyanate. 2. Infrared and mechanical studies. Macromolecules 1980; 13:117–121.
16. Meuse CW, Yang X, Yang D, Hsu SL. Spectroscopic analysis of ordering and phase-separation behavior of model polyurethanes in a restricted geometry. Macromolecules 1992;25: 925–932.
17. Coleman MM, Sobkowiak M, Pehlert GJ, Painter PC. Infrared temperature studies of a simple polyurea. Macromol Chem Phys 1997;198:117–136.
18. Manias E, Touny A, Wu L, Strawhecker K, Lu B, Chung TC. Polypropylene/montmorillonite nanocomposites: a review of synthetic routes and materials properties. Chem Mater 2001; 31:3516–3523.
19. Lincoln DM, Vaia RA, Wang ZG, Hsiao BS, Krishnamoorti RK. Temperature dependence of polymer crystalline morphology in nylon 6/montmorillonite nanocomposites. Polymer 2001;42: 9975–9985.
20. Wang Z, Pinnavaia TJ. Nanolayer reinforcement of elastomeric polyurethane. Chem Mater 1998;10:3769–3771.
21. Zilg C, Thomann R, Mülhaupt R, Finter J. Polyurethane nanocomposites containing laminated anisotropic nanoparticles derived from organophilic layered silicates. Adv Mater 1999;11:49–52.
22. Krishnamoorti R, Vaia RA, Giannelis EP. Structure and dynamics of polymer-layered silicate nanocomposites. Chem Mater 1996;8:1728–1734.
23. Cussler EL, Hughes SE, Ward WJ, Aria R. Barrier membranes. J Membr Sci 1988;38:161–174.
24. Fredrickson GH, Bicerano J. Barrier properties of oriented disk composites. J Chem Phys 1999;110:2181–2188.